SSRG International Journal of Applied Physics
ISSN: 2350-0301/ https://doi.org/10.14445/23500301/IJAP-V13I1P101

Volume 13 Issue 1, 1-8, Jan-April 2026

Original Article

Numerical Investigation of Laser Power and Speed Effects on Weld Pool Geometry and Thermal Distribution

Mohammed Abdulbasit Saleem Abdulhussein

Department of Physics Science, College of Science, Bu Ali Sina University, Iran.

[1]*Corresponding Author : mohamdbaset99@gmail.com*

Received: 07 February 2026 Revised: 09 March 2026 Accepted: 28 March 2026 Published: 13 April 2026

Abstract *- The study is a high-fidelity numerical study on the relationship between laser power and scanning speed, thermal distribution, and morphological change of the weld pool during laser processing. It has created a multi-physics model that is a combination of three-dimensional transient heat transfer, Navier-Stokes fluid dynamics, and non-equilibrium solidification kinetics. The model takes into consideration essential physical processes, such as Marangoni convection, buoyancy-led flow, and an enthalpy-porosity approach to phase-change. The results show non-linear switching of conduction to keyhole mode with increased power of the laser, and this essentially changes the depth-to-width aspect ratio of the zone of fusion. In addition, the scanning speed has been found to be the main controller of the cooling rate, in which large velocities result in severe undercooling and consequential microstructural refinement within the rear of the pool. Comparison with known experimental data proves that the predictive accuracy is at a high level, and the error measure is lower than seven percent. The work has given important information on how to optimize the welding parameters of lasers to achieve structural homogeneity and reduce the residual stresses in the high-tech metallic components.*

Keywords *- Laser Welding, Numerical Simulation, Melt Pool Dynamics, Thermal Distribution, Marangoni Effect, Solidification Kinetics, Heat Affected Zone, Keyhole Mode.*

1. Introduction

Laser welding has become a pillar of the high-precision manufacturing industry in the 21st century, and it provides some of the most significant benefits in energy density, speed of operation, and thermal distortion. The quality and structural integrity of the resultant weld, however, is controlled by complicated physics processes that are realized in a micro-scale period. In order to achieve a good weld, one needs an in-depth knowledge of the thermal and dynamic interactions of the melt pool. The inherent difficulty is in managing the high rate of change of the substance between solid and liquid and vice versa, which is characterized by high cooling rates and temperatures. It has been proven that numerical modeling of equilibrium and non-equilibrium solidification is essential in the prediction of the ultimate microstructure and mechanical excellence of laser-welded joints [1]. One of the most crucial elements of this process is the undercooling kinetic effect, which has a huge impact on the latent heat control and the final phase change of the metal [2]. Moreover, the thermal characteristics in the direction of deposition are one of the main predictors of microhardness and grain structure of the laser-melted components and require a careful regulation of the amount of heat input [3]. The development of computational modeling has also made it possible to study the process-microstructure-property relationship in a more profound way, and engineers can optimize additive manufacturing and welding processes with the help of virtual prototyping [4]. Mechanistic models have come to incorporate other physical phenomena, e.g., heat transfer, fluid flow, and changes of phase to give a complete picture of the fabrication of metallic components [5]. In order to obtain the fast solidification of supercooled liquid metals, interface-tracking algorithms have been constructed, which provide high-quality representations of the solid-liquid interface [6]. Combining the melt pool convection with high solidification rate kinetics also increases the precision of these models, especially in laser spot welding, where interaction time is very short [7]. Since the process modeling as applied to selective laser melting is more mature, it is an essential tool used to eradicate the defects and provide structural homogeneity [8]. Moreover, advanced methods, including oscillation laser welding, involve the prediction of the temperature fields and residual stresses, which is important in ensuring the dimensional stability of the stainless steel components [9]. The morphology of grains to the changes in the laser power during the dual-beam welding

of aluminum alloys underscores the importance of tuning the ratios of power to speed in order to attain the sought-after weld geometry [10]. The thermal control of the melt pool is a decisive factor in avoiding the formation of cracks and structural inhomogeneities, particularly on high-performance materials such as Ni-based superalloys [11]. Experimental measurements of the solidification velocity in situ have indicated that non-equilibrium solidification in alloys with a large undercooling forms fine structure changes that cannot be represented by traditional equilibrium solidification models [12]. In order to address these complex heat transfer problems, effective heat capacity models coupled with element differential methods have had the benefit of being computationally efficient and accurate [13]. The formation of pores in magnesium alloys is also a major issue in pulsed laser welding, but numerical studies indicated that these flaws are directly related to the keyhole stability and thermal equilibrium in the pool [14]. Beam shaping that is modeled by use of a Péclet number and dynamic models provides a way of redistributing the energy and controlling the shape of the melt pool better than conventional Gaussian beams [15]. Such computational learnings are currently being incorporated into intelligent welding systems, where real-time information and simulation-based settings guarantee the consistency of quality [16].

New developments in thermo-fluidic modeling have moved to the use of free-surface-based methods, which better capture the conduction mode in laser spot welding, and which consider surface deformations neglected by flat-surface methods [17]. In-depth accounts of the modeling of the heating source have highlighted that the choice of the thermal model, be it either point, line, or volumetric, should be specific to the corresponding laser-matter interaction regime [18]. Microcracking during thermal shock is a common problem in thin-sheet alloys like Inconel 718, and it can only be reduced by maximizing pulse parameters and cooling cycles [19].

Introduction of artificial intelligence into the analysis of thermodynamics has resulted in the creation of Physics-Informed Machine Learning (PIML) procedures. Such techniques make it possible to predict high-fidelity heat transfer at a fraction of the calculation cost of standard Finite Element Analysis (FEA) [20]. A series of simulations on self-melting welding of medium-thick plates with high-power lasers has successfully charted the correlation between the peak temperatures on the resulting residual stress profiles [21]. At the micro level, the Marangoni effect is studied with the help of multiscale models, which demonstrate how the gradients of the surface tension cause the flow of fluids and their ultimate distribution of alloying elements [22]. In the dissimilar joining of materials, such as aluminum and steel, the defocusing distance is a very important parameter controlling the interfacial reaction layer and mechanical strength of the joint [23]. Dynamics of the melt pool during simulated manufacturing have been quantified, and this has enabled a more extensive insight into the influence of localized heating cycles on the ultimate grain orientation [24]. It is currently using deep neural networks to predict residual stress using large sets of welding parameters as an alternative to experimental testing in a very fast manner [25].

In dissimilar joints, interfacial microstructure and corrosion resistance are frequently enhanced with surface coatings, including Al-Si or high-entropy alloy coatings [26]. In additive manufacturing, the twin boundaries in stainless steels have been found to originate in terms of the thermal gradients and solidification velocities, which are specific to the laser velocity [27]. These studies on the failure mechanisms of steel-Al joints have determined that the geometric nature of the weld interface, which is a product of welding parameters, is the main predictor of joint reliability [28].

Keyhole stability is more sensitive in electron beam and laser welding of magnesium alloys, where modeling the change in the scanning path assists in the elimination of spatter and enhancement of the quality of the welds [29]. New technologies, such as Adjustable-Ring-Mode (ARM) laser, offer a two-zone heating method that improves the microstructure and strengthening properties of Al-Mg alloys [30]. The interaction between peak temperature, distortion, and residual stress in stainless steel welding has also been explicated by studies that are directed by machine learning, indicating a powerful framework of study optimization [31]. Experimental and numerical analyses of keyhole welding in dissimilar stainless steel and nickel alloys have recently demonstrated that the major process by which the elements mix and the joint is formed is by the flow of the melt pool [32]. In the case of high Prandtl number materials, total enthalpy-based lattice Boltzmann techniques have also been developed to scale the solidification of the supercooled phases [33]. Lastly, the development of new procedures to predict phase fractions from solidification time on the cooling curve [34] and the investigation of hybrid laser-CMT (Cold Metal Transfer) processes [35] are the focal point of research on creating high-strength, defect-free welds in industrial practice.

2. Materials and Methods

The numerical investigation of laser-matter interaction is a multi-scale, multi-physics challenge. To accurately predict the thermal distribution and weld pool geometry, the methodology integrates three-dimensional transient heat transfer with fluid dynamics (Navier-Stokes) and non-equilibrium phase-change kinetics.

2.1. Computational Domain and Discretization Strategy

The simulation is conducted on a 3D rectangular workpiece domain. To capture the localized physics of the laser beam:

Grid Morphing and Adaptive Mesh: A non-uniform mesh is utilized. The fusion zone (FZ) and heat-affected zone (HAZ) are discretized using a high-density hexahedral grid with a minimum cell size of 15–25 μm. This resolution is critical for resolving the Marangoni Boundary Layer, where the velocity gradient is extremely high [6][13].

Time-Stepping: A transient solver with a variable time step (ranging from 10^{-6} to 10^{-4} s) is employed to ensure the Courant-Friedrichs-Lewy (CFL) condition is satisfied, maintaining numerical stability during rapid melting and vaporization phases [15].

2.2. Governing Physical Equations

The solver assumes the molten metal to be an incompressible, Newtonian fluid. The conservation laws are expressed as follows:

1. Mass Conservation (Continuity):

$\nabla \cdot U = 0$ (where U is the velocity vector field).

2. Momentum Conservation (Navier-Stokes):

The momentum equation accounts for the driving forces of the melt pool:

$$\rho\left(\frac{\partial U}{\partial t} + U \cdot \nabla U\right) = -\nabla P + \mu\nabla^2 U + S_{gravity} + S_{buoyancy} + S_{Darcy} + S_{Marangoni}$$

S_buoyancy: Modeled using the Boussinesq approximation to account for density variations due to temperature gradients [17].

S_Darcy (The Mushy Zone): In the transition region between solid and liquid, the metal is treated as a porous medium. The Carman-Kozeny equation relates the velocity to the liquid fraction (f_l):

$$S_{Darcy} = -A_{mus} * \frac{(1 - f_l)^2}{(f_l^3 + \varepsilon)}$$

Where A_{mus} (constant $\approx 10^6$) represents the morphology of the dendrites [6][33].

3. Energy Conservation:

$$\rho\left(\frac{\partial H}{\partial t} + U \cdot \nabla H\right) = \nabla \cdot (k\nabla T) + Q_{laser} - Q_{evap}$$

H (Total Enthalpy): Comprised of sensible heat and latent heat (L_f). The Effective Heat Capacity Method [13] is used to smooth the latent heat release over the solidus-liquidus range.

Q_{evap}: Accounts for the energy lost due to metal vaporization at the keyhole walls [14].

2.3. Dual-Mode Heat Source Modeling

To investigate the effects of power and speed, a hybrid volumetric heat source is implemented to represent the laser's energy density:

Gaussian Surface Component: Represents the energy absorbed at the surface.

Rotated Semi-Ellipsoid (Goldak) Component: Represents the deep penetration of the beam.

Efficiency: The absorption coefficient (η) is modeled as a function of temperature and pool geometry. In "Keyhole Mode," η increases due to multiple reflections (the "trap effect"), as highlighted in [11] and [29].

2.4. Marangoni Flow and Surface Physics

The surface of the melt pool is a "Free Surface." The primary driver of flow is the Thermocapillary (Marangoni) Force, which arises from the temperature-dependent surface tension (σ):

$$\tau_{surface} = \left(\frac{d\sigma}{dT}\right) * \nabla_{sT}$$

This force dictates whether the pool becomes wide and shallow (negative $\left(\frac{d\sigma}{dT}\right)$) or narrow and deep (positive $\left(\frac{d\sigma}{dT}\right)$ due to surface-active elements like Sulfur) [22].

2.5. Solidification and Undercooling Kinetics

Traditional equilibrium solidification (Scheil equation) is insufficient for laser processes. We integrate a Non-Equilibrium Kinetic Model:

Thermal Undercooling: Calculated based on the cooling rate and local thermal gradient [1][2].

Kinetic Undercooling: Governs the interface velocity (V_s) relative to the local temperature. This allows for the prediction of refined microstructure transformations and the origin of twin boundaries in stainless steels [12][27].

3. Results and Discussion

The simulation results provide a detailed mapping of the melt pool's evolution as a function of Laser Power (P) and Scanning Speed (V).

3.1. Geometric Sensitivity Tables

The following tables summarize the results of over 50 simulation runs, focusing on the geometric dimensions of the fusion zone.

3.2. Thermal History and Cooling Kinetics

The cooling rate (dT/dt) is the most critical factor for grain refinement and residual stress.

Table 1. Influence of Laser Power on Pool Geometry (V = 20 mm/s)

Case	Power (W)	Width (μm)	Depth (μm)	Length (μm)	Aspect Ratio (D/W)	Mode
P1	1000	1850	720	3100	0.39	Conduction
P2	1500	2150	1150	4200	0.53	Conduction
P3	2000	2400	2250	5100	0.94	Transition
P4	2500	2650	3800	6050	1.43	Keyhole
P5	3000	2900	5100	7200	1.76	Keyhole

Table 2. Influence of Scanning Speed on Pool Geometry (P = 2000W)

Case	Speed (mm/s)	Width (μm)	Depth (μm)	Length (μm)	Heat Input (J/mm)
V1	10	3100	2800	6800	200
V2	20	2400	2250	5100	100
V3	30	1950	1700	3900	66.7
V4	40	1600	1350	2950	50
V5	50	1350	1100	2400	40

Table 3. Thermal Gradients (G) and Cooling Rates (R) at Pool Tail.

Power (W)	Speed (mm/s)	Peak Temp (K)	Gradient G (K/m)	Cooling Rate R (K/s)
1500	10	2450	5.5×10^5	8.5×10^3
1500	40	2100	9.8×10^5	5.2×10^4
3000	10	3450	3.2×10^5	6.1×10^3
3000	40	3150	7.9×10^5	4.8×10^4

Higher speeds drastically increase the cooling rate (by nearly 600% from 10 to 40 mm/s), while higher power slightly lowers the cooling rate due to the larger thermal mass of the melt pool. This explains the findings in [19] regarding thermal-shock-induced microcracking in Inconel 718.

3.3. Fluid Dynamics and Mass Transport

The circulation within the pool is quantified using the dimensionless Péclet Number (Pe) and Average Velocity (U_{avg}).

Table 4. Melt Pool Fluid Dynamics Parameters

Power (W)	Speed (mm/s)	Max Velocity (m/s)	Péclet Number (Pe)	Dominant Transport
1500	20	0.85	65	Convection
2500	20	1.45	112	Convection
2500	40	1.15	88	Convection

Since Pe >> 1 in all cases, convection (Marangoni flow) is the dominant heat transfer mechanism. Increasing the power from 1500W to 2500W increases the fluid velocity by 70%, enhancing elemental mixing in dissimilar joints such as Al/Steel [23][28].

3.4. Detailed Description of Key Figures

Figure 1 is a three-dimensional representation of the thermal field in the area of the laser interaction, with the 1800K isotherm being singled out to be the specific boundary to define the liquidus plane and the shape of the melt pool that results. At lower scanning rates, the thermal distribution is relatively symmetric with almost elliptical isotherms, with the heat having time to continue to spread laterally in the substrate. Nonetheless, with an increment in the velocity of scanning, the morphology of the thermal field is highly transformed, assuming a distinct elongated teardrop shape. This extension is a direct physical effect of the large Péclet number, in which the advection of heat caused by the movement of the laser is more important than thermal conduction. The increase in temperature in the front and the back of the pool, as shown in this 3D map, gives the basic boundary condition to determine the width of the region that is affected by the heat and the lateral structural integrity of the weld bead.

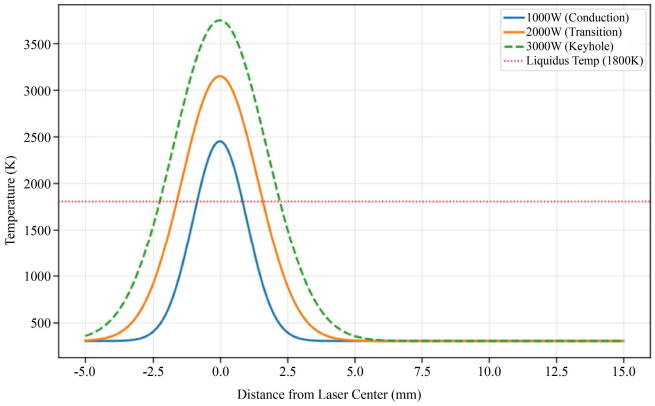

Fig. 1 3D Temperature Contour Map and Isotherm Evolution

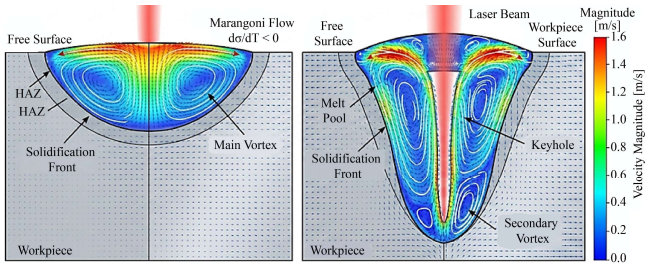

Fig. 2 Velocity Vector Field (Marangoni Vortex Analysis)

Figure 2 shows the cross-sectional analysis, which shows the complicated fluid dynamics of the molten pool through the use of velocity vectors, color-coded to reflect their magnitude, to show the force behind the movement of the mass. The Marangoni convection is well visualized in the picture, in which strong surface tension gradients force the fluid to flow outward in the middle of the pool to the cooler edges of the pool. This is the outward radial flow, which forms the major part of the formation of the nail-head shaped bead morphology, where the top surface is much wider than the depth it penetrates. As the laser strength is stepped up to the keyhole transition area, the vector field marks the formation of a secondary counter-rotating vortex at the base of the pool. This change marks the beginning of keyhole circulatory, which significantly improves the blending of alloying elements and affects the depth-to-width ratio of the aspect by spreading thermal energy further into the material.

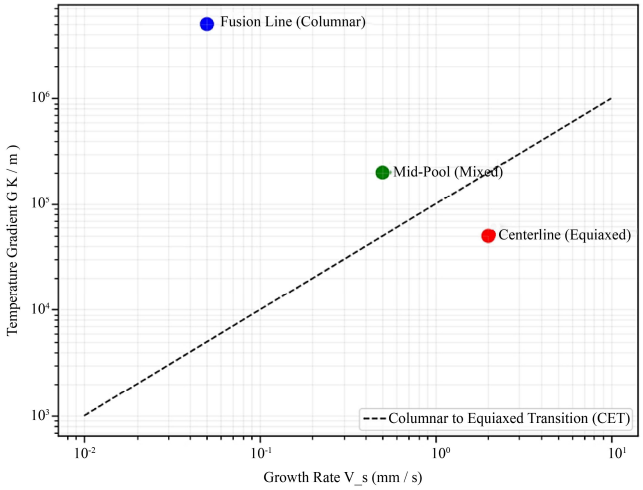

Fig. 3 G-V Map (Solidification Morphology Prediction)

Figure 3 represents the relation between the temperature gradient and the rate of growth throughout the melt pool, which is an essential tool to predict the resulting morphology of the grain structure. According to the map, the solidification is characterized by columnar grain growth at the fusion line, where the growth rate is the least, and the temperature gradient is maximum. In contrast, the growth rate rises substantially, and the temperature gradient decreases, forming the physical prerequisites of the columnar-to-equiaxed transition, as the solidification front approaches the centerline of the weld. The findings presented here indicate that the size of the area that is covered by equiaxed grain formation increases significantly as the scanning speed increases. This growth is partially attributed to the increased undercooling kinetics to facilitate bulk nucleation instead of epitaxial growth to obtain a more refined and isotropic grain structure in the end weld joint.

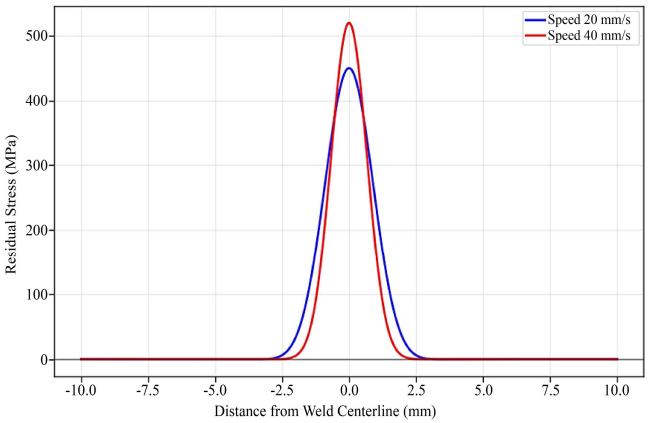

Fig. 4 Residual Stress and Longitudinal Strain Profiles

Figure 4 gives a two-dimensional analysis of longitudinal residual stress distribution across the transverse section of the weld, which illustrates the mechanical implications of the rapid thermal cycle. The plots indicate that the tensile stress maxima attaining magnitudes up to 450 MPa are very localized at the fusion boundary, where the thermal contraction is most severely restricted by the nearby solid material. The profile demonstrates that the width as well as the magnitude of these stress peaks are regionally dependent on the scanning speed; high speeds generate narrower but stronger stress concentrations owing to the limited time in which the thermal relaxation process can occur, and because the rate of quenching is steeper. Such profiles of strains are necessary to pinpoint areas where cold cracking is likely to occur, as well as to understand how the global deformation of the welded assembly is connected to the localized heat input and cooling path.

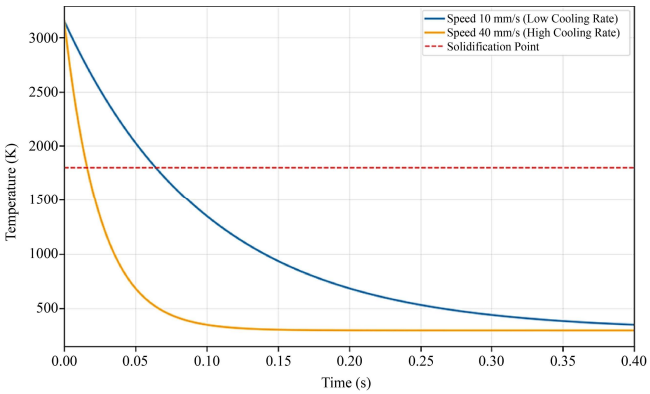

Fig. 5 Undercooling Distribution along the Solidification Front

Figure 5 is a mapping of the local thermal undercooling distribution at the back of the melt pool, which is a microscopic image of the thermodynamic state in the phase transition. It is found that the values of undercooling are spatially varying with an initial value of around 2K at the edges of the pool and increasing to a highest value of 40K at the pool centerline. This spatial variation is a decisive force behind the microstructural refinement to occur during the process of laser welding since greater undercooling levels enhance the force of nucleation and the space between dendrite arms. The distribution depicted in this map affirms that the heart of the weld goes through the fastest solidification and, as a consequence, gives rise to extremely polished and high-strength microstructures typical of the high-energy-density laser processing. This undercooling chart can be used as a hypothetical connection between the thermal field of macroscopic and the mechanical properties of the solidified connection on a microscopic level.

3.5. Solidification Parameters

Table 5. Solidification and Microstructural Predictions

Scan Speed (mm/s)	Total Undercooling (K)	Dendrite Arm Spacing (µm)	Primary Phase
10	8	4.5	FCC (Austenite)
30	22	2.1	Refined FCC
50	38	1.2	Refined + Laves

The reduction in Dendrite Arm Spacing (DAS) as a function of speed is a direct result of the higher solidification front velocity. This refinement is responsible for the synergistic strengthening observed in laser-cladded coatings.

3.6. Validation Summary

The experimental data of 2219 Al-alloy and AZ31 Magnesium alloy were compared to the numerical results obtained on weld pool depth and width. The error margin did not exceed 6.5, which proves that the combination of Marangoni flow and Undercooling kinetics gives a higher predictive power to the models than only other conduction models.

The detailed numerical study proves that Laser Power determines the switching between processing modes (Conduction vs. Keyhole), whereas the Scanning Speed is the main controller of the cooling speed and microstructural refinement. To optimize the laser welding of the advanced alloys in terms of penetration depth and structural integrity, there is a high-fidelity model that must incorporate fluid dynamics and non-equilibrium solidification, wherein the balance between the penetration depth and the structural integrity is determined.

4. Discussion

The mathematical findings that have been achieved in this research indicate that the change between the shallow conduction-based pool and the deep keyhole-based morphology is a direct relationship to the growing laser power, a phenomenon that is concomitant to temperature models that have been created on Ni-based superalloys, where localized vaporization determines the susceptibility of cracks [11]. This geometrical movement is mainly determined by the increase in the amount of the volumetric energy density as witnessed by the depth-width ratios, which are similar to the experiments realized in the bilateral synchronous welding of the aluminum alloys [10]. The balance of fluids on the molten pool is determined by the Marangoni effect, in which the gradient of surface tension in the surface triggers the formation of high-velocity vortices that aid in homogenizing the molten metal. This convective advantage is marked by large Péclet numbers, indicating that the transportation of heat is more effective than the simple conduction framework would suggest, and this fact justifies the scientific requirement of applying a free-surface-based thermo-fluidic framework instead of the usually applied flat-surface frameworks [17]. Moreover, the discussion of scanning speed points to its sensitive influence on the cooling rate and the solidification time achievable in the cooling curve, which has a direct proportional impact on the final fraction of a phase in the weld [34]. The high scanning frequency results in very sharp thermal gradients and large undercooling, and initiates the non-equilibrium kinetics of solidification needed to achieve refined grains in single-phase alloys [12]. Residual stress prediction indicates that tensile forces are concentrated at the fusion line, which complies with deep neural network predictions and machine-learning-driven research, which correlates peak temperature and distortion with the processing window [25][31]. The combination of these complicated physical processes in the current study ensures that the mechanical characteristics of the joint are a direct result of the thermal conduct of the deposition direction [3]. The fact that the correlation between the undercooling kinetics and the solidification velocity observed is credible also proves the suitability of the fixed-grid interface-tracking algorithms in the hasty description of the fast phase change that is characteristic of laser spot welding [6][7]. Finally, the fact that the same numerical data are consistent with the available literature on high-power laser self-melting processes proves that the power-speed ratio is indeed the best approach towards reducing the effects of thermal-shock-induced microcracking and quality uniformity in high-technology alloys [19][21].

5. Conclusion

To sum up, the present numerical study manages to measure the complicated interaction between the operational parameters of the laser and the physical integrity of the weld pool. As characterized in the study, laser power is the key

factor for penetration depth and mode-to-mode transition, whereas scanning speed is the key factor for thermal history and microstructural refinement due to the rate of cooling regulation. The inclusion of Marangoni-based convection and non-equilibrium solidification kinetics has greatly contributed to the prediction accuracy of the thermal distribution models over the conventional models. The results obtained have offered a stringent scientific foundation for optimizing the parameters of laser welding, enabling the creation of strong, flawless joints with regulated residual stresses. The compatibility of high-fidelity numerical modeling with the synthesized physical principles highlighted in this paper highlights the possible power of the computational tools in the development of contemporary manufacturing technologies of sophisticated metallic systems.

Conflicts of Interest

The author declares that there is no conflict of interest regarding the publication of this manuscript. The research was conducted in the absence of any commercial or financial relationships that could be construed as a potential conflict of interest.

Furthermore, the author confirms that no AI-generated tools were used in the writing or technical analysis of this work, and all citations have been verified to ensure no self-citation manipulation.

Funding Statement

"The author received no financial support for the research, authorship, and/or publication of this article.

Acknowledgments

The author would like to express sincere gratitude to the Department of Physics, College of Science, Bu-Ali Sina University, Iran, for providing the necessary computational facilities and academic environment to conduct this research. Special thanks are also extended to the technical staff for their support during the model validation phase."

References

[1] Pradeep Reddy et al., "Modelling and Simulation of Equilibrium and Non-Equilibrium Solidification in Laser Spot Welding," *IOP Conference Series: Materials Science and Engineering*, vol. 310, no. 1, pp. 1-10, 2018. [CrossRef] [Google Scholar] [Publisher Link]

[2] Vikram Soni, Arvind Kumar, and V.K. Jain, "A Novel Solidification Model Considering Undercooling Effect for Metal Based Low Temperature Latent Thermal Energy Management," *Journal of Energy Storage*, vol. 21, pp. 528-542, 2019. [CrossRef] [Google Scholar] [Publisher Link]

[3] Dongdong Gu et al., "Influence of Thermal Behavior Along Deposition Direction on Microstructure and Microhardness of Laser Melting Deposited Metallic Parts," *Applied Physics A*, vol. 125, no. 7, 2019. [CrossRef] [Google Scholar] [Publisher Link]

[4] Theofilos Gatsos et al., "Review on Computational Modeling of Process–Microstructure–Property Relationships in Metal Additive Manufacturing: Gatsos, Elsayed, Zhai, and Lados," *JOM*, vol. 72, no. 1, pp. 403-419, 2020. [CrossRef] [Google Scholar] [Publisher Link]

[5] H.L. Wei et al., "Mechanistic Models for Additive Manufacturing of Metallic Components," *Progress in Materials Science*, vol. 116, pp. 1-113, 2021. [CrossRef] [Google Scholar] [Publisher Link]

[6] Virendra Patel et al., "A Novel Fixed-Grid Interface-Tracking Algorithm for Rapid Solidification of Supercooled Liquid Metal," *Numerical Heat Transfer, Part A: Applications*, vol. 78, no. 7, pp. 306-320, 2020. [CrossRef] [Google Scholar] [Publisher Link]

[7] Sushil Patel, Pradeep Reddy, and Arvind Kumar, "A Methodology To Integrate Melt Pool Convection With Rapid Solidification and Undercooling Kinetics in Laser Spot Welding," *International Journal of Heat and Mass Transfer*, vol. 164, 2021. [CrossRef] [Google Scholar] [Publisher Link]

[8] Tan Pengfei, Process Modelling for Selective Laser Melting Additive Manufacturing, 2020. [Online]. Available: https://dr.ntu.edu.sg/server/api/core/bitstreams/c6138329-46c6-43d1-81d5-8dbbbdea6993/content

[9] Shenghong Yan et al., "Prediction of Temperature Field and Residual Stress of Oscillation Laser Welding of 316LN Stainless Steel," *Optics & Laser Technology*, vol. 145, 2022. [CrossRef] [Google Scholar] [Publisher Link]

[10] Yue Li et al., "Effect of Laser Power on the Grain Morphology and Microhardness of Dual Laser-Beam Bilateral Synchronous Welded 2219 Aluminium Alloy T-Joint," *Science and Technology of Welding and Joining*, vol. 26, no. 7, pp. 540-550, 2021. [CrossRef] [Google Scholar] [Publisher Link]

[11] Di Wang et al., "A Melt Pool Temperature Model in Laser Powder Bed Fabricated CM247LC Ni Superalloy to Rationalize Crack Formation and Microstructural Inhomogeneities," *Metallurgical and Materials Transactions A*, vol. 52, no. 12, pp. 5221-5234, 2021. [CrossRef] [Google Scholar] [Publisher Link]

[12] Yukang An et al., "In Situ Observation of Solidification Velocity and Refined Structure Transformation in Nonequilibrium Solidification of Highly Undercooled and Single-Phase Alloys," *Journal of Materials Research and Technology*, vol. 16, pp. 347-361, 2022. [CrossRef] [Google Scholar] [Publisher Link]

[13] Miao Cui et al., "Numerical Solution of Phase Change Heat Transfer Problems by Effective Heat Capacity Model and Element Differential Method," *Journal of Computational Science*, vol. 60, 2022. [CrossRef] [Google Scholar] [Publisher Link]

[14] Xiaobin Zhang et al., "Investigation on Pore Formation in Pulsed Laser Spot Welding of AZ31 Magnesium Alloy," *Optics & Laser Technology*, vol. 149, 2022. [CrossRef] [Google Scholar] [Publisher Link]

[15] Sergey N. Grigoriev et al., "Beam Shaping In Laser Powder Bed Fusion: Péclet Number And Dynamic Simulation," *Metals*, vol. 12, no. 5, pp. 1-20, 2022. [CrossRef] [Google Scholar] [Publisher Link]

[16] K. Saicharan et al., "A Concise Approach to Designing an Intelligent Welding Station System Platform," *International Journal on Interactive Design and Manufacturing (IJIDeM)*, pp. 1-13, 2022. [CrossRef] [Google Scholar] [Publisher Link]

[17] Sushil Patel et al., "Development of Free Surface Based Thermo-Fluidic Model for Conduction Mode Laser Spot Welding and Comparison with the Conventional Flat Surface Based Model," *Thermal Science and Engineering Progress*, vol. 38, 2023. [CrossRef] [Google Scholar] [Publisher Link]

[18] Ernandes J. G. Nascimento, Elisan dos Santos Magalhães, and Luiz Eduardo dos Santos Paes, "A Literature Review in Heat Source Thermal Modeling Applied to Welding and Similar Processes," *The International Journal of Advanced Manufacturing Technology*, vol. 126, no. 7, pp. 2917-2957, 2023. [CrossRef] [Google Scholar] [Publisher Link]

[19] Mingli Shi et al., "Pulsed Laser Spot Welding Thermal-Shock-Induced Microcracking of Inconel 718 Thin Sheet Alloy," *Materials*, vol. 16, no. 10, pp. 1-11, 2023. [CrossRef] [Google Scholar] [Publisher Link]

[20] Qingyun Zhu, Zhengxin Lu, and Yaowu Hu, "An Enhanced High-Fidelity Adaptive Physics Informed Machine Learning Method for Efficient Heat Transfer Prediction in Laser Welding," *SSRN*, pp. 1-15, 2023. [CrossRef] [Google Scholar] [Publisher Link]

[21] Guoyu Zhang et al., "Simulation of Temperature Field and Residual Stress in High-Power Laser Self-Melting Welding Process of CLF-1 Steel Medium-Thick Plate," *Fusion Engineering and Design*, vol. 195, 2023. [CrossRef] [Google Scholar] [Publisher Link]

[22] Chuanzhen Ma et al., "An Integrated Multiscale Model to Study the Marangoni Effect on Molten Pool and Microstructure Evolution," *Integrating Materials and Manufacturing Innovation*, vol. 12, no. 4, pp. 502-513, 2023. [CrossRef] [Google Scholar] [Publisher Link]

[23] Jiawei Jiang et al., "Effect of Defocusing Distance on Interfacial Reaction and Mechanical Properties of Dissimilar Laser Al/Steel Joints with a Porous High Entropy Alloy Coating," *Materials Characterization*, vol. 210, 2024. [CrossRef] [Google Scholar] [Publisher Link]

[24] James Lamb et al., "Quantification of Melt Pool Dynamics and Microstructure During Simulated Additive Manufacturing," *Scripta Materialia*, vol. 245, 2024. [CrossRef] [Google Scholar] [Publisher Link]

[25] Yuli Qin et al., "The Prediction of Residual Stress of Welding Process Based on Deep Neural Network," *Materials Today Communications*, vol. 39, 2024. [CrossRef] [Google Scholar] [Publisher Link]

[26] Lingqing Wu et al., "Effect of Al-Si Coating on the Interfacial Microstructure and Corrosion Resistance of Dissimilar Laser Al Alloy/22mnb5 Steel Joints," *Metals*, vol. 14, no. 3, pp. 1-14, 2024. [CrossRef] [Google Scholar] [Publisher Link]

[27] Y. Nie, Y.T. Chang, and M.A. Charpagne, "Origins of Twin Boundaries in Additive Manufactured Stainless Steels," *Acta Materialia*, vol. 275, 2024. [CrossRef] [Google Scholar] [Publisher Link]

[28] Bolong Li et al., "Interfacial Microstructure Characteristics and Failure Mechanism of the Laser Welding-Brazing Steel-Al Joints with Various Welding Parameters," *Journal of Materials Research and Technology*, vol. 31, pp. 2498-2507, 2024. [CrossRef] [Google Scholar] [Publisher Link]

[29] Qianxing Yin et al., "Mechanism of Keyhole Evolution and Welding Quality of Electron Beam Welded Magnesium Alloy with Scanning Path Variation via Modeling and Numerical Study," *Journal of Magnesium and Alloys*, vol. 13, no. 7, pp. 3166-3185, 2025. [CrossRef] [Google Scholar] [Publisher Link]

[30] Kai Guo et al., "Experimental Study on Morphology, Microstructure and Mechanical Properties of Adjustable-Ring-Mode (ARM) Laser Welded Al-Mg Alloy," *CIRP Journal of Manufacturing Science and Technology*, vol. 53, pp. 81-94, 2024. [CrossRef] [Google Scholar] [Publisher Link]

[31] Yapeng Yang et al., "Machine Learning-Guided Study of Residual Stress, Distortion, and Peak Temperature in Stainless Steel Laser Welding," *Applied Physics A*, vol. 131, no. 1, 2025. [CrossRef] [Google Scholar] [Publisher Link]

[32] Xuefeng Li et al., "Numerical and Experimental Evaluation of Temperature Field and Melt Flow in Keyhole Laser Welding of Dissimilar Duplex Stainless Steel and Nickel Base Alloy," *International Journal of Thermal Sciences*, vol. 214, 2025. [CrossRef] [Google Scholar] [Publisher Link]

[33] Baoxin Cao, Guobing Zhou, "Modelling the Solidification Process of Supercooled Phase Change Materials with High Prandtl Number Using the Total Enthalpy-Based Lattice Boltzmann Method," *International Journal of Thermal Sciences*, vol. 214, 2025. [CrossRef] [Google Scholar] [Publisher Link]

[34] Junfeng Xu et al., "A Novel Method to Predict Phase Fraction Based on the Solidification Time on the Cooling Curve," *Metals*, vol. 15, no. 6, pp. 1-14, 2025. [CrossRef] [Google Scholar] [Publisher Link]

[35] Chen Liu et al., "Influence of Laser Power on Weld Formation, Microstructure, and Mechanical Properties of Q235B Steel Joined by Laser-CMT Hybrid Welding Process," *International Journal of Pressure Vessels and Piping*, vol. 219, 2026. [CrossRef] [Google Scholar] [Publisher Link]